11. K. A. Farley, *Nature* **376**, 153 (1995).
12. _____, S. G. Love, D. B. Patterson, *Geochim. Cosmochim. Acta* **61**, 2309 (1997).
13. S. G. Love and D. E. Brownlee, *Science* **262**, 550 (1993).
14. S. Dermott *et al.*, in *Physics, Chemistry and Dynamics of Interplanetary Dust*, B. Gustafson and M. Hanner, Eds. (Astronomical Society of the Pacific, San Francisco, CA, 1996), vol. 104, pp. 143–153.
15. D. B. Patterson, K. A. Farley, B. Schmitz, in preparation.
16. S. Amari and M. Ozima, *Nature* **317**, 520 (1985).
17. I. Premoli-Silva, R. Coccioni, A. Montanari, Eds., *The Eocene-Oligocene Boundary in the Marche-Umbria Basin (Italy)* (International Union of Geological Sciences, Ancona, Italy, 1988).
18. Limestone samples of ~2.5 g were dried at 90°C overnight, powdered, sieved, and dissolved in 10% acetic acid. After complete decarbonation, the residue was isolated, dried, weighed (to obtain the noncarbonate fraction), and transferred to a tinfoil packet. The packet was fused in vacuum, and the evolved He was purified and analyzed by mass spectrometry (*11*). The estimated analytical uncertainty on [^{3}He] and ^{3}He/^{4}He determinations is <3%. We report [^{3}He] per gram of bulk limestone. In some cases, replicate analyses were made; the mean value is plotted.
19. S. Dermott, P. Nicholson, J. Burns, J. Houck, *Nature* **312**, 505 (1984).
20. F. Marzari, D. Davis, V. Vanzani, *Icarus* **113**, 168 (1995).
21. J. C. Liou, S. F. Dermott, Y. L. Xu, *Planet. Space Sci.* **43**, 717 (1995).
22. P. Weissman, *Nature* **344**, 825 (1990).
23. J. Hills, *Astron. J.* **86**, 1730 (1981); P. Weissman, *Earth Moon Planets* **72**, 25 (1996).
24. M. Rampino and R. Stothers, *Nature* **308**, 709 (1984).
25. J. Liou and H. Zook, *Icarus* **123**, 491 (1996).
26. R. Grieve and L. Pesonen, *Earth Moon Planets* **72**, 357 (1996).
27. S. A. Vishnevsky and A. Montanari, in preparation.
28. O. Pierrard, E. Robin, R. Rocchia, A. Montanari, *Geology* **26**, 307 (1998).
29. J. J. Matese, P. G. Whitman, K. A. Innanen, M. J. Valtonen, *Icarus* **116**, 255 (1995).
30. L. Lanci, W. Lowrie, A. Montanari, *Earth Planet. Sci. Lett.* **143**, 37 (1996).
31. We thank P. Weissman for a constructive and thoughtful review and D. Patterson and K. Robinson for assistance with sample preparation. Supported by NASA and by the David and Lucille Packard Foundation through a fellowship award to K.A.F.

13 January 1998; accepted 27 March 1998

Fullerene Pipes

Jie Liu, Andrew G. Rinzler, Hongjie Dai, Jason H. Hafner, R. Kelley Bradley, Peter J. Boul, Adrian Lu, Terry Iverson, Konstantin Shelimov, Chad B. Huffman, Fernando Rodriguez-Macias, Young-Seok Shon, T. Randall Lee, Daniel T. Colbert, Richard E. Smalley*

Single-wall fullerene nanotubes were converted from nearly endless, highly tangled ropes into short, open-ended pipes that behave as individual macromolecules. Raw nanotube material was purified in large batches, and the ropes were cut into 100- to 300-nanometer lengths. The resulting pieces formed a stable colloidal suspension in water with the help of surfactants. These suspensions permit a variety of manipulations, such as sorting by length, derivatization, and tethering to gold surfaces.

Single-wall carbon nanotubes (SWNTs) of molecular perfection—fullerene nanotubes—are of great interest because of their unique electronic (*1*) mechanical (*2*) properties combined with chemical stability. The present availability of various fullerene structures reveals a large gap in the intermediate size range between small spheroidal fullerenes and long SWNTs. This intermediate size range could, however, be of paramount scientific and technological importance. For example, fullerene tubes in the length range of 10 to 300 nm might provide connectors and components for molecular electronic devices. We report here methods that make available, in substantial quantities, fullerene macromolecules occupying this intermediate length range. Our approach involves cutting the nearly endless, highly tangled ropes of nanotubes that are currently available (*3*, *4*) into short lengths of open tubes—fullerene pipes—so they can be suspended, sorted, and manipulated as individual macromolecules.

A vital step in developing the molecular science and technology of these fullerene macromolecules is to take advantage of the rich chemistry available at their ends. We also report here the rational derivatization of these fullerene pipes. The ongoing elaboration of these structures should result in a class of organic molecules with the potential for broad applications.

The SWNTs for this study were prepared by a scaled-up version (*5*) of the laser-oven method described previously (*3*, *6*). Although this method produces fullerene nanotube material of lower quality (50%) than the previously described method (70 to 90%), it has the advantage of being able to produce 20 g of material in 2 days of continuous operation. This as-grown material contains a substantial fraction of nanoscale impurities (bucky onions, spheroidal fullerenes, amorphous carbon, and others) that are difficult to separate from the nanotubes once they have been cut. For this reason, it became imperative that the starting material be purified before cutting. Previously reported purification methods for multiwalled carbon nanotubes (MWNTs) (*7*) and SWNTs (*8*) either totally destroy or are ineffective at purifying the present SWNT material in large amounts. Ultimately, we developed a purification method that consists of refluxing in 2.6 M nitric acid and resuspending the nanotubes in pH 10 water with surfactant followed by filtration with a cross-flow filtration system (*9*).

Passing the resultant purified SWNT suspension through a polytetrafluoroethylene filter produced a free-standing mat of tangled SWNT ropes—a "bucky paper." Typical scanning electron microscope (SEM) images near and at a torn edge of a paper are shown in Fig. 1, B and C, respectively. As is evident in Fig. 1C, the tearing process produces a substantial alignment of the SWNT ropes. The net yield of purified fullerene fibers from this method depends on the initial quality of the raw material, with typical yields in the range of 10 to 20% by weight. A particularly low-quality starting material (Fig. 1A) was chosen to highlight the efficacy of the method. Survival of such a high percentage of these fibers after refluxing for days in nitric acid is indicative of the high degree of molecular perfection of their sidewalls.

Extensive SEM and transmission electron microscope imaging of the fullerene rope fibers in these purified samples shows them to be highly tangled with one another and so long that their ends are rarely visible. The frequent occurrence of fullerene toroids ("crop circles") in these samples (*10*) suggests that fullerene rope ends are hard to find because many of the ropes are, in fact, truly endless. We suspect that this condition results from van der Waals adherence of the "live" ends of the ropes to the sides of other ropes as growth proceeds in the argon atmosphere of the laser-oven method. The growing rope ends are then eliminated in collisions with other live rope ends growing along the same guiding rope from the opposite direction. In one dimension, collisions are unavoidable.

We verified that one can cut and make ends from these tangled, nearly endless ropes by several techniques ranging from simply cutting with a pair of scissors to

J. Liu, A. G. Rinzler, H. Dai, J. H. Hafner, R. K. Bradley, P. J. Boul, A. Lu, T. Iverson, K. Shelimov, C. B. Huffman, F. Rodriguez-Macias, D. T. Colbert, R. E. Smalley, Center for Nanoscale Science and Technology, Rice Quantum Institute, Departments of Chemistry and Physics, Rice University, Houston, TX 77005, USA.
Y.-S. Shon and T. R. Lee, Department of Chemistry, University of Houston, Houston, TX 77204, USA.

*To whom correspondence should be addressed. E-mail: res@cnst.rice.edu

bombardment with relativistic gold ions. However, a far more effective and efficient method was prolonged sonication of the nitric acid–purified SWNT rope material in a mixture of concentrated sulfuric and nitric acids (3:1, 98% and 70%, respectively) at 40°C (*11*).

We infer that this method is effective because the collapse of cavitation bubbles in ultrasonication produces microscopic domains of high temperature (*12*), leading to localized sonochemistry that attacks the surface of the SWNT tubes, leaving an open hole in the tube side. There are previous reports that vigorous sonication in CH_2Cl_2 can damage the sides of MWNTs (*13*), but the goal here with the SWNT ropes was not just to damage the tubes but to cut them cleanly at the points of damage and separate the cut pieces from the other tubes in the ropes. The advantage of sonicating in the presence of an oxidizing acid is that subsequent attack at the point of damage soon cuts the tube completely. Because at these moderate temperatures the open tube ends are unable to close, continued exposure to the oxidizing acid then slowly etches away the exposed ends, much like the burning of a fuse.

The 3:1 concentrated H_2SO_4:HNO_3 mixture was chosen for the oxidizing acid in this cutting operation because it is also known to intercalate and exfoliate graphite (*14*). We suspected that it may similarly help to separate the cut tube pieces from the underlying tubes in the rope, thereby exposing these inner SWNTs to new sonication-induced damage and subsequent further cutting. As shown in Fig. 2, the result is efficient cutting of the SWNT rope material into thinned rope pieces and individual cut tubes (*15*).

To ensure that the cut nanotube pieces were themselves molecularly perfect and chemically clean, we subjected them to further etching in acid without sonication. As expected for open-ended tubes, that is, fullerene pipes, the length distribution shortened systematically with exposure time to the acid. For example, in 3:1 concentrated sulfuric and nitric acid at 70°C, we found that the average cut nanotube shortened at a rate of roughly 130 nm $hour^{-1}$ (Fig. 3). At 70°C in a mixture of concentrated sulfuric acid and 30% aqueous hydrogen peroxide (4:1 by volume), the shortening rate was roughly 200 nm $hour^{-1}$. As advances in sorting nanotubes by helical type are made, it will be interesting to determine whether this etching rate is sensitive to the chiral indices of the nanotubes (n, m), for example, whether all "armchair" tubes ($n = m$) have a distinct chemistry from "zigzag" tubes ($m = 0$) and from those of the intermediate helical angle.

The purified SWNT nanotubes flocculated rapidly in aqueous solution, hindering their further manipulation and analysis. We found that stable colloidal suspensions in

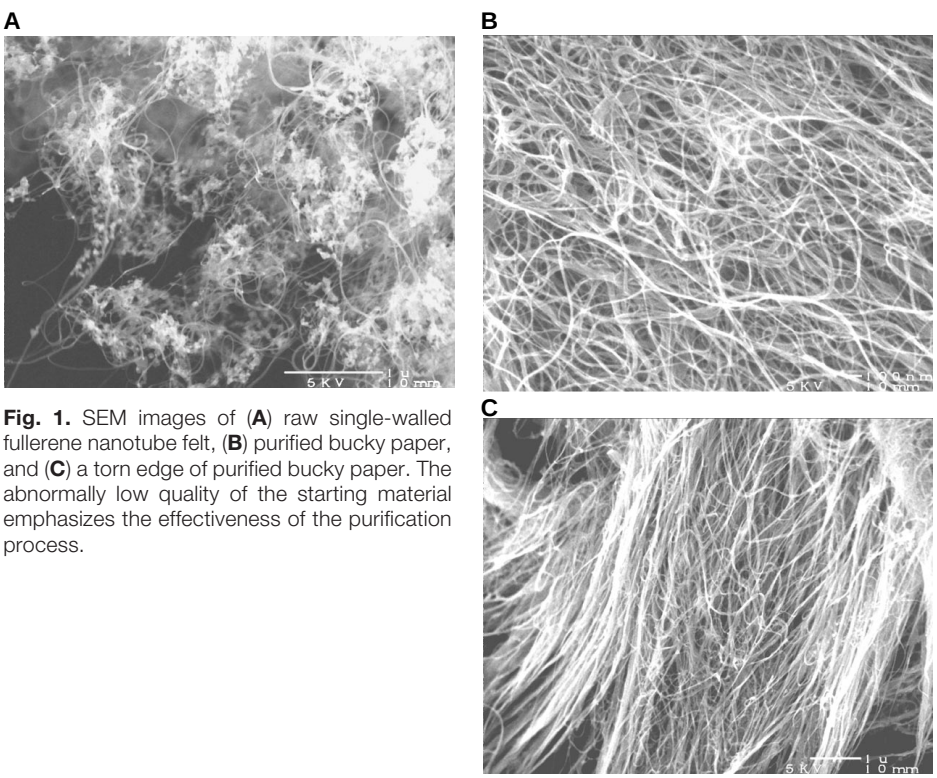

Fig. 1. SEM images of (**A**) raw single-walled fullerene nanotube felt, (**B**) purified bucky paper, and (**C**) a torn edge of purified bucky paper. The abnormally low quality of the starting material emphasizes the effectiveness of the purification process.

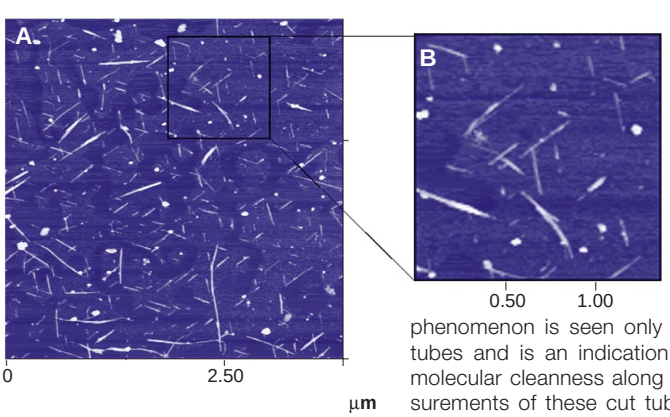

Fig. 2. (**A** and **B**) Tapping mode AFM images of cut fullerene nanotubes (pipes) electrodeposited from a stable colloidal suspension onto HOPG. Note the tendency of tubes to align 120° to one another, presumably in registry with the underlying graphite lattice. This phenomenon is seen only with well-purified fullerene tubes and is an indication of a very high degree of molecular cleanness along the tube sides. AFM measurements of these cut tubes show that roughly half have heights corresponding to individual tubes (1 to 2 nm), whereas the rest are aggregates of several tubes in van der Waals contact.

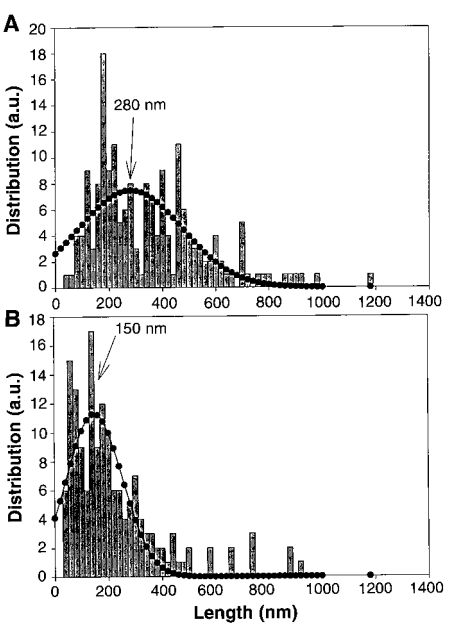

Fig. 3. Size distribution plots of cut nanotubes (**A**) before and (**B**) after stirring in a 3:1 mixture of sulfuric and nitric acid at 70°C for 1 hour. The average length before acid treatment was 280 nm (A), and the average length afterward was 150 nm (B). a.u., arbitrary units.

water could be made for cut nanotubes with the assistance of anionic surfactants such as sodium dodecyl sulfate or the nonionic surfactant Triton X-100.

Figure 4 demonstrates the use of these stable nanotube suspensions to achieve a separation by length with field-flow fractionation (FFF) (*16*), with subsequent analysis by AFM imaging. To ensure that we deposited a representative sample of nanotubes from solution, we developed an electrodeposition technique that drives essentially all nanotubes in suspension onto the surface of highly oriented pyrolytic graphite (HOPG), which was subsequently scanned by atomic force microscope (AFM) (*17*). This technique relies on the fact that nanotubes readily pick up negative charges in aqueous suspension (*18*).

As a demonstration of the molecular nature of these cut fullerene pipes, we proceeded to derivatize them at their open ends. Presuming these open ends to be terminated with many carboxylic acid groups as a result of previous treatment in acid (*19*), we converted these groups to the corresponding acid chloride by reaction with $SOCl_2$ at room temperature. Subsequent exposure to NH_2-$(CH_2)_{11}$-SH in toluene at room temperature produced an amide linkage of the nanotube to the alkanethiol. We assayed this chemistry by using the free thiol end to tether the end of the nanotube to a 10-nm diameter gold particle. AFM imaging revealed that most tubes derivatized in this way have a single gold particle bound to at least one of their ends, as demonstrated in Fig. 5. Similar results were obtained regardless of whether the gold particles were exposed to the tubes before or after being deposited on HOPG. Control experiments verified that derivatization was necessary: Gold particles were seldom found at the ends of tubes without alkanethiol tethers. Attachment of such strategically designed binding groups may be very useful in directing assembly of fullerene tubes into molecular devices.

AFM imaging of the cut nanotube pieces on HOPG shows that many are individuals but that many remain in van der Waals contact with each other, perhaps having started as partners in the original rope material. The filtration methods used here discard the most interesting nanotubes: those with lengths substantially less than 100 nm. As we approach this 100-nm length from above, we are beginning to enter the realm of fullerene molecules whose chemistry and physics are dominated by their ends. Although the cut tube pieces made here are open pipes, we expect that they will be closed by true hemifullerene end caps, forming sealed fullerene capsules, simply by annealing in vacuum at 1000° to 1200°C. The ready rearrangement of carbon sheets to incorporate pentagons, curve, and close at these temperatures is the dominant chemical physics that produces the fullerenes in the first place. Open or closed, these fullerene tubes will have a rich chemistry. They are the fitting subject of a new branch of organic chemistry, a molecular technology of great promise.

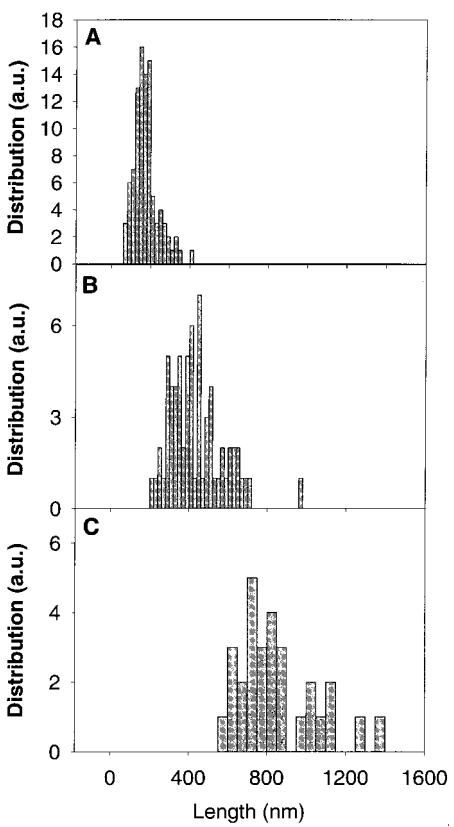

Fig. 4. FFF of cut fullerene nanotube "pipes" in aqueous suspension. (**A** to **C**) Nanotube length distributions as measured from AFM images of the suspended fullerene nanotubes electrodeposited on HOPG, as in Fig. 2, for earlier and later FFF fractions.

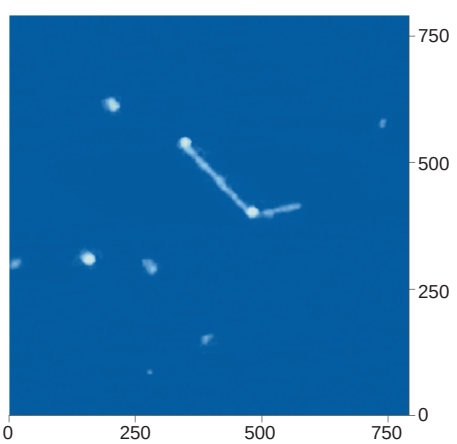

Fig. 5. "Seven minutes to three": an AFM image of two "fullerene pipes" tethered to a common 10-nm-diameter gold sphere. The longer pipe (the minute hand) has another gold particle tethered to its other end. The image was taken after the tubes were electrodeposited onto HOPG from a suspension of a mixture of derivatized tubes with colloidal gold particles (Sigma) in water. The nanotube-to-gold tethers were constructed of alkyl thiol chains attached by amide linkages to open tube ends previously derivatized by converting terminating carboxylic acid groups (arising from the acidic cutting treatment) to the corresponding acid chloride by reaction with $SOCl_2$. Scale in nanometers.

REFERENCES AND NOTES

1. S. J. Tans *et al.*, *Nature* **386**, 474 (1997).
2. E. W. Wong, P. E. Sheehan, C. M. Lieber, *Science* **277**, 1971 (1997); B. I. Yakobson and R. E. Smalley, *Am. Sci.* **85**, 324 (1997).
3. A. Thess *et al.*, *Science* **273**, 483 (1996).
4. C. Journet *et al.*, *Nature* **388**, 756 (1997).
5. A. G. Rinzler *et al.*, *Appl. Phys. A*, in press.
6. T. Guo, P. Nikolaev, A. Thess, D. T. Colbert, R. E. Smalley, *Chem. Phys. Lett.* **243**, 49 (1995).
7. Y. J. Chen *et al.*, *Adv. Mater.* **8**, 1012 (1996); T. W. Ebbesen, P. M. Ajayan, H. Hiura, K. Tanigaki, *Nature* **367**, 519 (1994).
8. K. Tohji *et al.*, *J. Phys. Chem. B* **101**, 1974 (1997); K. Tohji *et al.*, *Nature* **383**, 679 (1996).
9. In a typical procedure, a raw sample of nanotubes (8.5 g) was first refluxed in 1.2 liters of 2.6 M nitric acid for 45 hours. Upon cooling, the solution was transferred to polytetrafluoroethylene centrifuge tubes and spun at 2400*g* for 2 hours. The supernatant acid was decanted off, replaced by deionized water, and vigorously shaken to resuspend the solids, followed by a second centrifuge-decant cycle. The solids were resuspended in 1.8 liters of water with 20 ml of Triton X-100 surfactant (Aldrich) and adjusted to pH 10 with sodium hydroxide. The suspension was then transferred to the reservoir of a tangential flow filtration system (MiniKros Lab System; Spectrum, Laguna Hills, CA). The filter cartridge used (M22M 600 01N; Spectrum) had mixed cellulose ester hollow fibers of 0.6-mm diameter, 200-nm pores, and a total surface area of 5600 cm^2. The buffer consisted of 44 liters of 0.2 volume % Triton X-100 in water, of which the first 34 liters were made basic (pH 10) with sodium hydroxide and the final 10 liters were at pH 7. The cartridge inlet pressure was maintained at 6 psi. A control valve was added to the exit so that the outflow rate was restricted to 70 ml min^{-1}.
10. J. Liu *et al.*, *Nature* **385**, 780 (1997).
11. These cut tubes were prepared in a two-step process: cutting and polishing. In a typical example, 10 mg of the purified SWNT "bucky paper" (Fig. 1B) was suspended in 40 ml of a 3:1 mixture of concentrated H_2SO_4/HNO_3 in a 100-ml test tube and sonicated in a water bath [Cole Palmer (Verona Hills, IL) model B3-R, 55 kHz] for 24 hours at 35° to 40°C. The resultant suspension was then diluted with 200 ml of water, and the larger cut SWNTs were collected on a 100-nm pore filter membrane (type VCTP; Millipore) and washed with 10 mM NaOH solution. The cut tubes were then further polished by suspension in a 4:1 mixture of concentrated H_2SO_4:30% aqueous H_2O_2 and stirring at 70°C for 30 min. After filtering and washing again on a 100-nm pore filter, the cut nanotubes were suspended at a density of 0.1 mg/ml in water with the aid of 0.5 weight % Triton X-100 surfactant.
12. T. J. Mason and J. P. Lorimer, *Sonochemistry: Theory, Applications and Uses of Ultrasound in Chemistry* (Halsted, New York, 1988).
13. K. L. Lu *et al.*, *Carbon* **34**, 814 (1996).
14. S. F. McKay, *J. Appl. Phys.* **35**, 1992 (1964).
15. Taking into account AFM tip broadening, the possibility remains that some of these apparent individual tubes are actually "rafts" of several parallel tubes in van der Waals contact lying on the HOPG surface.
16. A 20-μl sample of cut nanotube suspension (0.07 mg/ml) in 0.5% aqueous Triton X-100 was injected

into an FFF instrument (Model F-1000-FO, FFFractionation; LLC, Salt Lake City, UT) operating with 0.007% Triton X-100 in water mobile phase at 2 ml min^{-1} and a cross-flow rate of 0.5 ml min^{-1}.
17. Electrodeposition was performed by placing 20 μl of the nanotube suspension on the surface of a freshly cleaved HOPG substrate (Advanced Ceramics, Cleveland, OH), confining the droplet within a viton O-ring (4-mm outer diameter, 1.7 mm thick), capping the trapped suspension with a stainless steel electrode on top of the O-ring, and applying a steady voltage of 1.1 V for 6 min. When suspended in water, the nanotubes are negatively charged and are therefore driven by the electric field onto the HOPG surface. After deposition, the HOPG-nanotube surface was washed with methanol on a spin coater to remove the water and Triton X-100 surfactant.
18. K. Bubke, H. Gnewuch, M. Hempstead, J. Hammer, M. L. H. Green, *Appl. Phys. Lett.* **71**, 1906 (1997); A. G. Rinzler and R. E. Smalley, unpublished data.
19. K. Kinoshita, *Carbon Electrochemical and Physicochemical Properties* (Wiley, New York, 1988), pp. 199–201.
20. We thank K. Smith and V. Colvin for helpful discussions. Supported by the NSF, the Office of Naval Research, the Advanced Technology Program of Texas, and the Robert A. Welch Foundation.

12 January 1998; accepted 27 March 1998

Cloned Transgenic Calves Produced from Nonquiescent Fetal Fibroblasts

Jose B. Cibelli, Steve L. Stice, Paul J. Golueke, Jeff J. Kane, Joseph Jerry, Cathy Blackwell, F. Abel Ponce de León, James M. Robl*

An efficient system for genetic modification and large-scale cloning of cattle is of importance for agriculture, biotechnology, and human medicine. Here, actively dividing fetal fibroblasts were genetically modified with a marker gene, a clonal line was selected, and the cells were fused to enucleated mature oocytes. Out of 28 embryos transferred to 11 recipient cows, three healthy, identical, transgenic calves were generated. Furthermore, the life-span of near senescent fibroblasts could be extended by nuclear transfer, as indicated by population doublings in fibroblast lines derived from a 40-day-old fetal clone. With the ability to extend the life-span of these primary cultured cells, this system would be useful for inducing complex genetic modifications in cattle.

Research has been in progress for more than a decade to develop a system for genetic modification and large-scale cloning in cattle (*1*), an important species in agriculture, biotechnology, and human medicine. In the initial work on cloning, embryonic blastomeres were used as donor nuclei because they were thought to be relatively undifferentiated, readily reprogrammed, and likely to support full-term development of the fetus (*2*). Initial efforts at refining the methodology of nuclear transfer resulted in significant, but limited, improvements in efficiency, and at most, only a few identical calves could be produced from a single donor embryo because of the limited number of cells in the early embryo (*3*). The next step toward expanding the potential of cloning was the development and use of embryonic stem cells as a source of donor nuclei. Embryonic stem cells are derived from the inner cell mass of an early embryo and are thought to be relatively undifferentiated. In addition, mouse embryonic stem cells divide indefinitely in culture without differentiation and can be readily genetically modified (*4*). Embryonic stemlike cells have been developed in the bovine (*5*) and have been used as a source of donor nuclei in nuclear transfer, but they only supported development of fetuses to 60 days in vivo (*6*). To date, a source of cells that can be used for genetic modification and large-scale cloning in cattle has not been found.

Other research in nuclear transplantation has shown that the cell cycle stage of the donor cell affects the extent of development of the embryo after nuclear transfer. When the donor cell is fused to the recipient oocyte, which is arrested in the second metaphase in meiosis, the nuclear envelope breaks down and the chromosomes condense until the oocyte is activated (*7*). This condensation phase has been shown to cause chromosomal defects in donor cells that are undergoing DNA synthesis (*7*). Donor cells in the G_1 phase of the cell cycle (before DNA synthesis), however, condense normally and support a high rate of early development (*7*).

In previous work in the sheep, it was suggested that arrest in G_0 (by serum starvation) was the key in allowing donor somatic cells to support development of embryos to term (*8*).

Our rationale in selecting an optimal donor cell for nuclear transplantation was that the cell should not have ceased dividing (which is the case in G_0) but be actively dividing, as an indication of a relatively undifferentiated state and for compatibility with the rapid cell divisions that occur during early embryo development. The cells should also be in G_1, either by artificially arresting the cell cycle or by choosing a cell type that has an inherently long G_1 phase. We chose fibroblasts from fetuses because they can grow rapidly in culture and have an inherently long G_1 phase (*9*).

Fetal fibroblasts were isolated from a day 55 male fetus (Fig. 1A), cultured in vitro, and passaged twice before being transfected with a marker construct consisting of a β-galactosidase–neomycin resistance fusion gene driven by a cytomegalovirus (CMV) promoter (pCMV/β-GEO) (*10*). Cells were selected with neomycin for 2 weeks, and five neomycin-resistant colonies were isolated and analyzed for stable transfection by polymerase chain reaction (PCR) amplification of a segment of the transgene (*11*) and by assay of β-galactosidase activity. Colony CL1 was chosen for nuclear transfer experiments. These fibroblast cells

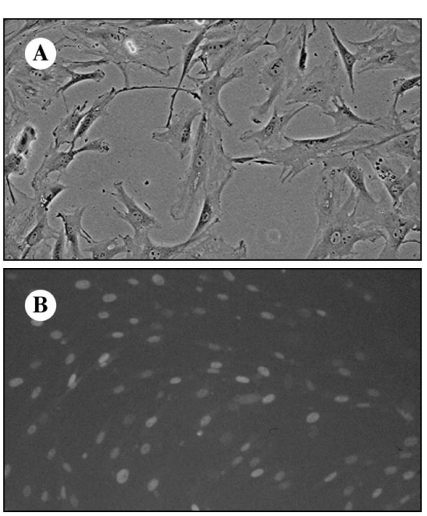

Fig. 1. Transgenic fetal fibroblast CL1-5 used for nuclear transplantation (**A**) phase contrast (×100). (**B**) Labeling of CL1-5 fibroblast cell line with PCNA monoclonal antibody (Sigma, St. Louis, MO) and FITC-conjugated secondary antibody (magnification × 200).

J. B. Cibelli, J. Jerry, J. M. Robl, Department of Veterinary and Animal Sciences, University of Massachusetts, Amherst, MA 01003, USA.
S. L. Stice, P. J. Golueke, J. J. Kane, C. Blackwell, Advanced Cell Technology, Incorporated, One Innovation Drive, Worcester, MA 01605, USA.
F. A. Ponce de León, Animal Sciences, College of Agricultural, Food and Environmental Sciences, 1404 Gortner Avenue, St Paul, MN 55108, USA.

*To whom correspondence should be addressed. E-mail: robl@vasci.umass.edu